InSAR Maps Peatlands in the Waikato Region of New Zealand

Mark Harvey[a] and Clint Rissmann[b]

[a]Harvey Geoscience Ltd, New Zealand; [b]Land and Water Science Ltd, New Zealand

Harvey Geoscience Ltd, 29 Ridge Rd, Mahurangi East, Warkworth, New Zealand

mark@harveygeoscience.com

Land and Water Science Ltd, 77 Marama Ave South, Otatara, Southland, New Zealand

InSAR Maps Peatlands in the Waikato Region of New Zealand

We use remote sensing techniques to assess regional-scale ground deformation in the Waikato Region of New Zealand. Interferometric Synthetic Aperture Radar (InSAR) is applied to measure surface deformation from 2018 to 2022, while digital elevation model (DEM) differencing provides elevation change data from 2013 to 2021. Both methods reveal subsidence within previously mapped peat soil boundaries, confirming ongoing loss of peat soil. InSAR time series show seasonal surface oscillations, aligning with ground-based observations from the same period. The primary driver of subsidence is the artificial drainage of peatlands for agriculture with significant environmental implications for soil conservation, climate change mitigation, water quality, and flood risk management. Our findings demonstrate that satellite-based approaches offer an efficient and scalable method for monitoring peatland subsidence across broad regions, which is not feasible with ground-based methods alone. More moderate subsidence is also observed in low-relief, flood-prone areas beyond the peatlands including the Hauraki Plains, though further validation is needed.

Keywords: InSAR, subsidence, LiDAR, satellite, DEM, Waikato, soil, peat.

Introduction

Interferometric Synthetic Aperture Radar (InSAR) is a remote sensing method that utilises satellite-based radar to investigate ground surface deformation. InSAR was previously used in New Zealand to evaluate deformation related to hydrothermal activity and magmatism (Hamling et al., 2016; Hamling, 2020; Harvey, 2021), tectonic processes (Hamling et al., 2022), and slope creep in steep rural terrain, caused by seasonal swelling/shrinking behaviour of clay-rich soils (Cook et al., 2023), and vertical land motion over coastal strips in New Zealand, using Sentinel-1 InSAR and GNSS data (Kearse, 2024).

Here we use LiCSBAS an open-source package to carry out InSAR time series analysis using LiCSAR products (July 2018 to July 2022) across 8,000 km^2 of mostly low relief pastural land in the Waikato Region of New Zealand. LiSCAR data products are made available by the Centre for Observation and Modelling of Earthquakes, Volcanoes and Tectonics (COMET), and their suitability for measurement of soil deformation in grasslands was previously demonstrated. For example, Xu et al. (2022) measured regional-scale surface deformation of permafrost in the Qinghai–Tibet Plateau, an area covered by alpine meadows, grasslands and deserts, and Orhan et al. (2023) identified widespread (~40,000 km^2) subsidence in the grasslands and croplands Konya Basin, Türkiye, resulting from agricultural groundwater usage.

We also use DEM differencing, comparing an older satellite-based DEM (2013 Copernicus 30m) to a newer LiDAR DEM (2021), to validate LiCSBAS results. DEM differencing was previously used to provide confirmation of InSAR subsidence maps in Taupo, New Zealand (Harvey et al., 2019).

Historically, New Zealand was dominated by forest below the alpine treeline, but about 1000 years of Polynesian and European colonisation has resulted in the destruction of nearly three-quarters of the indigenous forest cover (Ewers et al., 2006). As of 2024 approximately 52.5% of the land area of the Waikato Region is covered by high producing exotic grassland (LCDB5, http://www.lris.scinfo.org.nz), mostly utilised for dairy farming and livestock grazing.

New Zealand once had approximately 1660 km^2 of peat wetlands, around 0.7% of the total land surface area. Of this, approximately 940 km^2 was in the Waikato Region (*Figure 1*). Over 80% of Waikato peatlands have now been drained for pastoral use (since the early 1900s) (Davoren, 1978; Pronger et al., 2014; Layton, 2022). This has resulted in widespread ongoing subsidence from soil densification and loss of carbon through oxidation of organic matter (19–34 mm year^{-1}) (Schipper and McLeod, 2002; Pronger et al., 2014; Glover-Clark, 2020). However, drainage is not limited to peatlands, being widespread throughout low relief areas of Waikato in soils with variable organic carbon content, and related subsidence may be widespread.

Drainage benefits agriculture because it allows the soil to drain sooner after heavy rain, increasing grazing days and soil respiration, which improves productivity (Monaghan, 2004). The main environmental impacts of drainage are i) soil shrinkage and subsidence, ii) acceleration of lateral subsurface contaminant flow from land to water (Pearson, 2015), and iii) oxidation of organic matter (soil nutrient loss and increased CO_2 emissions to the atmosphere) (Schipper and McLeod, 2002; Pronger et al., 2014, Glover-Clark, 2020; Layton, 2022). InSAR has been utilised elsewhere to measure surface motion of drained peatlands as these soils are particularly important sources of atmospheric CO_2 (Alshammari et al., 2020; Hoyt et al., 2020; Tampuu et al., 2023; Hrysiewicz et al., 2024).

Soil subsidence incurs direct economic costs for farmers; the need to deepen drains continually to match the rate of subsidence further lowers the water table, perpetuating a drainage–subsidence cycle (Pronger et al., 2014). The economic productivity of soils can be lost if they sink below sea level or if the underlying mineral layer is unsuitable for agriculture (Ingebritsen et al., 1999; Pronger et al., 2014). Progressive deepening of drains and streams is also implicated in stream bank erosion, enhancing sediment loss rates in developed catchments (Blann et al. 2009).

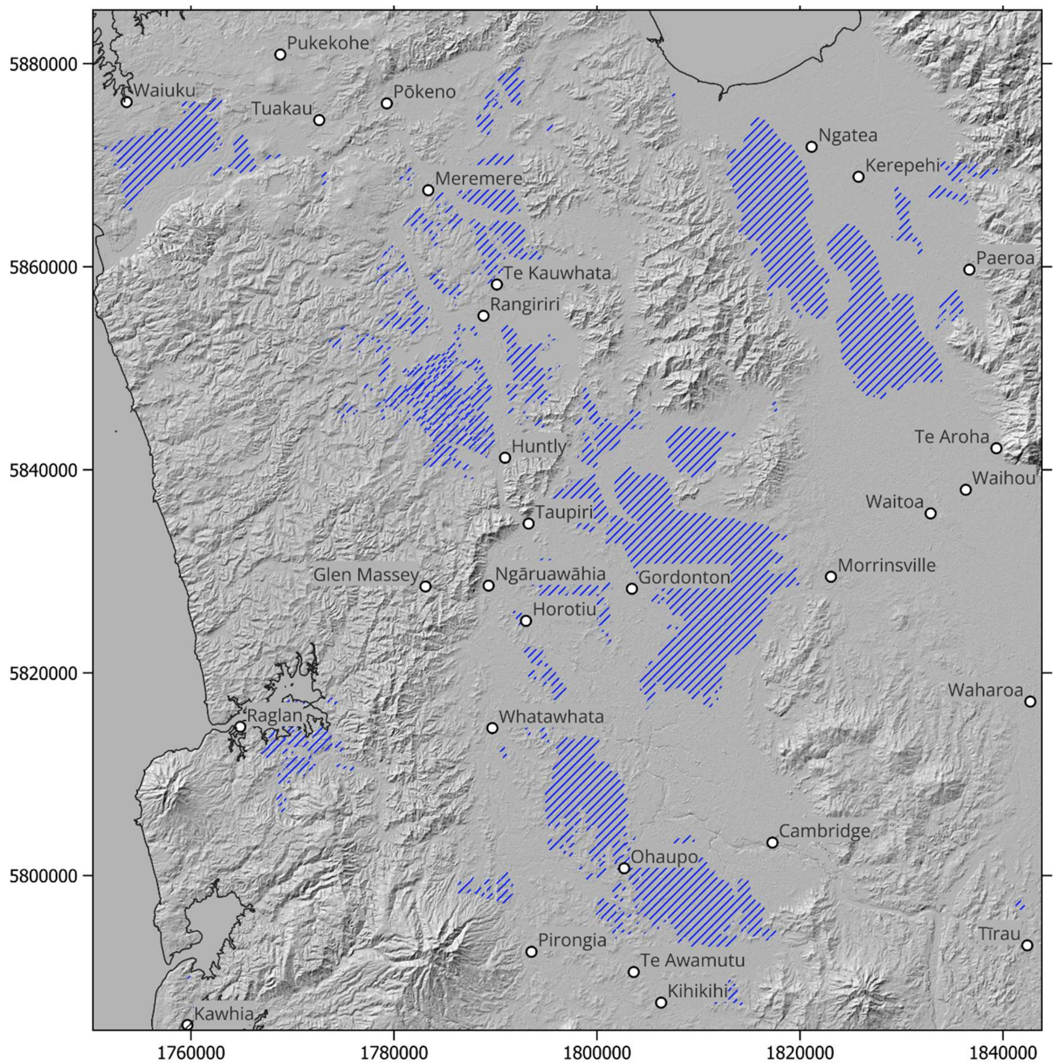

Figure 1. Waikato study location overlaid on SRTM DEM (Farr & Kobrick, 2000). Cross hatching indicates peat soil areas (https://lris.scinfo.org.nz/layer/119585-s-map-soil-classification-soilorder-aug-2024/).

Methods

For subsidence mapping and time series plotting we use LiCSBAS, a semi-automated InSAR time series analysis package that interfaces with the automated Sentinel-1 InSAR processor (LiCSAR) (Morishita et al., 2020). LiCSBAS processes publicly available LiCSAR data to undertake InSAR time series processing. An advantage of LiCSBAS is loop closure, a quality control process whereby interferograms with many unwrapping errors are automatically identified and discarded. LiCSBAS was run using masking parameters chosen by trial and error to provide a balance between good coverage in grassland areas, while masking dense forest with low coherence (*Figure 2*).

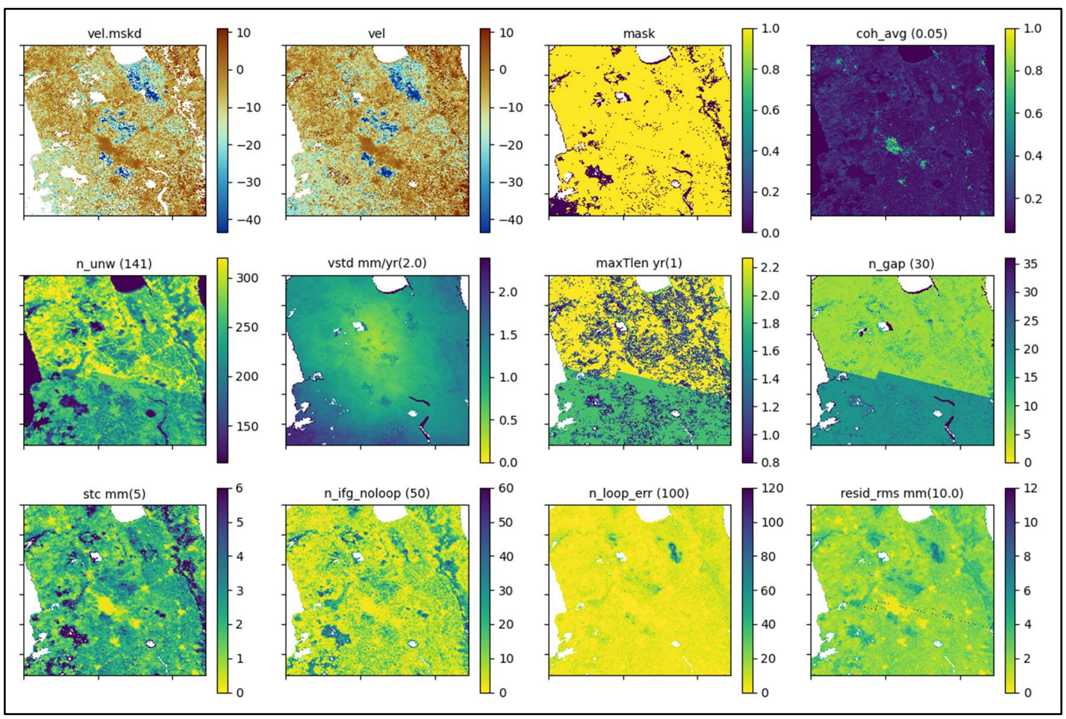

Figure 2. LiCSBAS masking parameters. Numbers shown in the parentheses next to the titles of each noise index are the applied threshold value. See Morishita et al. (2020) for full explanation of masking thresholds.

Time series for LOS results were obtained using the LiCSBAS interactive time series viewer that provides both filtered and unfiltered series for any selected pixel. For time series in this report, red cumulative displacement points and curves represent unfiltered results, whilst those shown in blue have a spatial filter of 2 km and a temporal filter of ~40 days applied. Filtering helps to reduce noise and highlight seasonal patterns. The viewer automatically fits sinusoidal curves to the time series to show seasonal cycles.

For the Waikato, the LiCSBAS dataset was limited to the descending orbit only (complete ascending data not available for the area/time of interest). Deformation is assumed to result from near-vertical subsidence in peatland areas (Layton, 2022; Pronger et al., 2014; Schipper and McLeod, 2002). Estimation of vertical motion uses the approach of Manzo (2006) (*eq. 2*), simplified for the single line-of-sight (LOS) viewing geometry:

$$dz \approx dLOS / \cos \theta \qquad (1)$$

Where dLOS is LOS motion from the descending pass, and θ is the average elevation angle (radians) for the study area.

The period 9th of July 2018 to 30th June 2022 included 111 Sentinel-1 acquisitions, with 466 interferograms available from the COMET-LiCS portal for approximately 8,000 km^2 of the Waikato Region (*Figure 1*). Of these 146 were automatically discarded from further processing by the LiCSBAS loop closure quality control process, leaving a network of 320 interferograms.

Small temporal baseline methods including LiCSBAS may be subject to the ‘fading signal’ processing artifact, which can confound results by mimicking and subsidence in cropland environments (Maghsoudi et al., 2022). The uncertainty introduced by this, and the single orbit viewing perspective means deformation rates mapped in this study have unknown precision and may be exaggerated in areas with grass and crops. Despite these uncertainties, LiCSBAS may still permit useful mapping of relative rates, i.e. to determine if elevated subsidence is associated with known peat soil boundaries.

An additional deformation map was obtained using an independent method and dataset; DEM differencing was undertaken between i) an Copernicus satellite based DEM from 2013 (average elevation 2011 - 2015 with vertical accuracy ± <2m for slopes below 20%) (https://dataspace.copernicus.eu/explore-data/data-collections/copernicus-contributing-missions/collections-description/COP-DEM; accessed 01/01/2025), and ii) a LiDAR DEM captured between 5 January and 26 March 2021 (vertical accuracy of ± 0.2m) (https://data.linz.govt.nz/layer/113203-waikato-lidar-1m-dem-2021/; accessed 01/01/2025).

As for LiCSBAS, DEM differencing also has uncertainties; the vertical precision of the Copernicus DEM (<2m) is large compared to the expected annual rates of deformation (10's of mm $year^{-1}$), and the acquisition date (2011 – 2015) means the DEM provides average of elevations in that time period. But just as with LiCSBAS, the approach may still permit useful mapping of relative rates.

All reported motions are relative to a reference location on the town of Cambridge that is assumed to be stable (all towns in the Waikato are observed to be stable). Summary statistics (mean and standard deviation) were extracted from the vertical velocity map using QGIS Zonal Statistics. Map grid units are meters (NZTM 2000). Map grid units are meters (NZTM 2000).

Results

Mapped InSAR results show strong subsidence within 708 km^2 of peat soil boundaries (*Figure 3*). Pixels selected from with these boundaries (n = 6.4×10^4) averaged -31 mm $year^{-1}$ (LOS) for the 2018 – 2022 period. Assuming the LOS measurements result from vertical subsidence provides an average rate of ~ -40 mm $year^{-1}$ (*Eq. 1*) for the peatlands, and ~ -25 mm $year^{-1}$ for the Hauraki Plains. DEM differencing (2013 Copernicus versus 2021 LiDAR) confirms the subsidence within peat soil boundaries for all southern peatlands, and widespread subsidence in surrounding low-elevation farmland, including the Hauraki Plains (*Figure 4*).

Time series for selected peatland locations and non-peat soil on the Hauraki Plains (numbered point locations in *Figure 3*) show well-defined seasonal surface oscillations superimposed on a longer-term subsidence trend (*Figure 5*).

Waikato time series were noted to contain many gaps after mid-2020 (see vertical lines in *Figure 5* time series), especially in the southern half of the study area, which derives from a separate Sentinel-1 burst. These gaps divide the series into discrete segments that LiCSBAS aligns by assuming an overall linear displacement trend (Morishita et al., 2020). This process provides good alignment of segments, at least for selected time series in *Figure 5*.

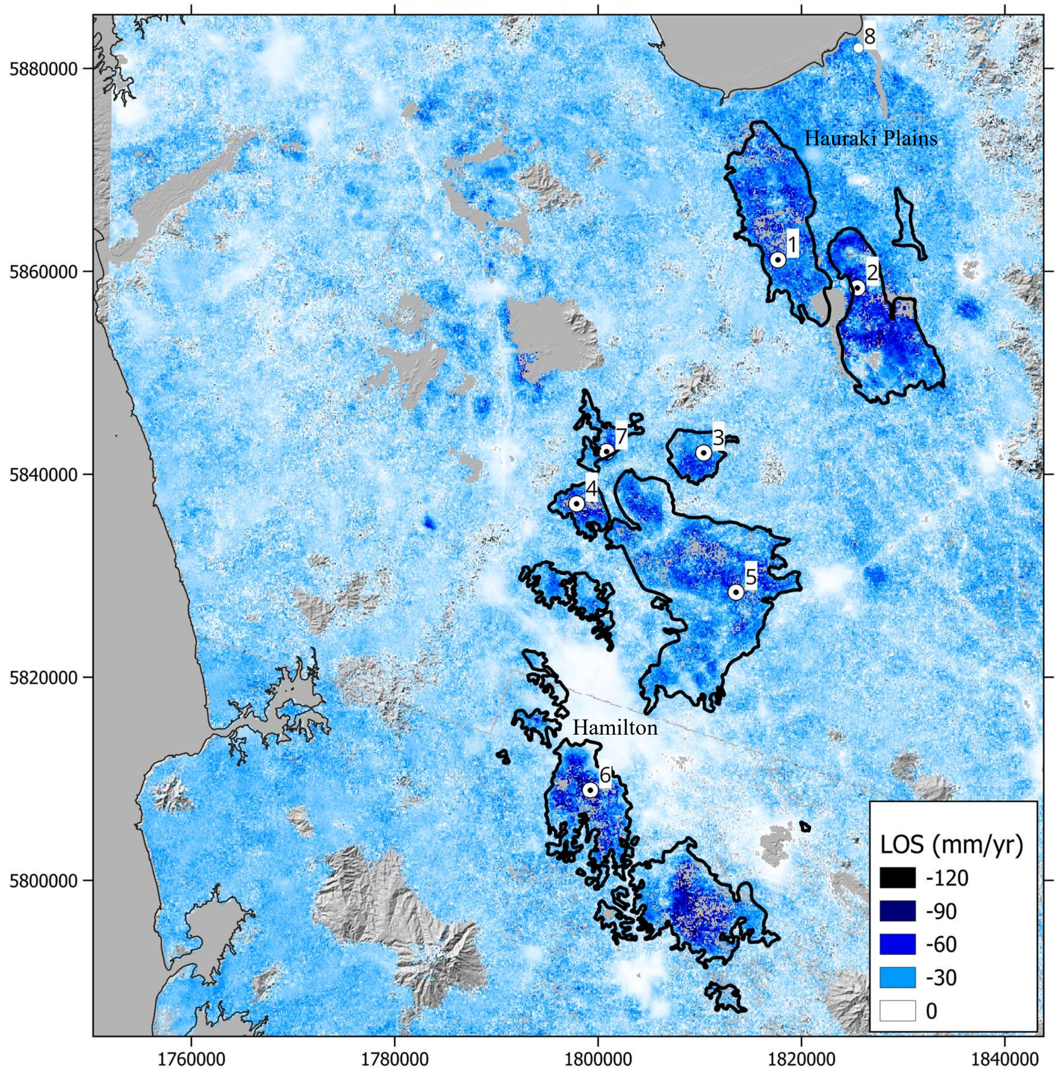

Figure 3. InSAR velocity map showing subsidence associated with peat soils (black boundaries). Numbers show time series locations (Figure 5).

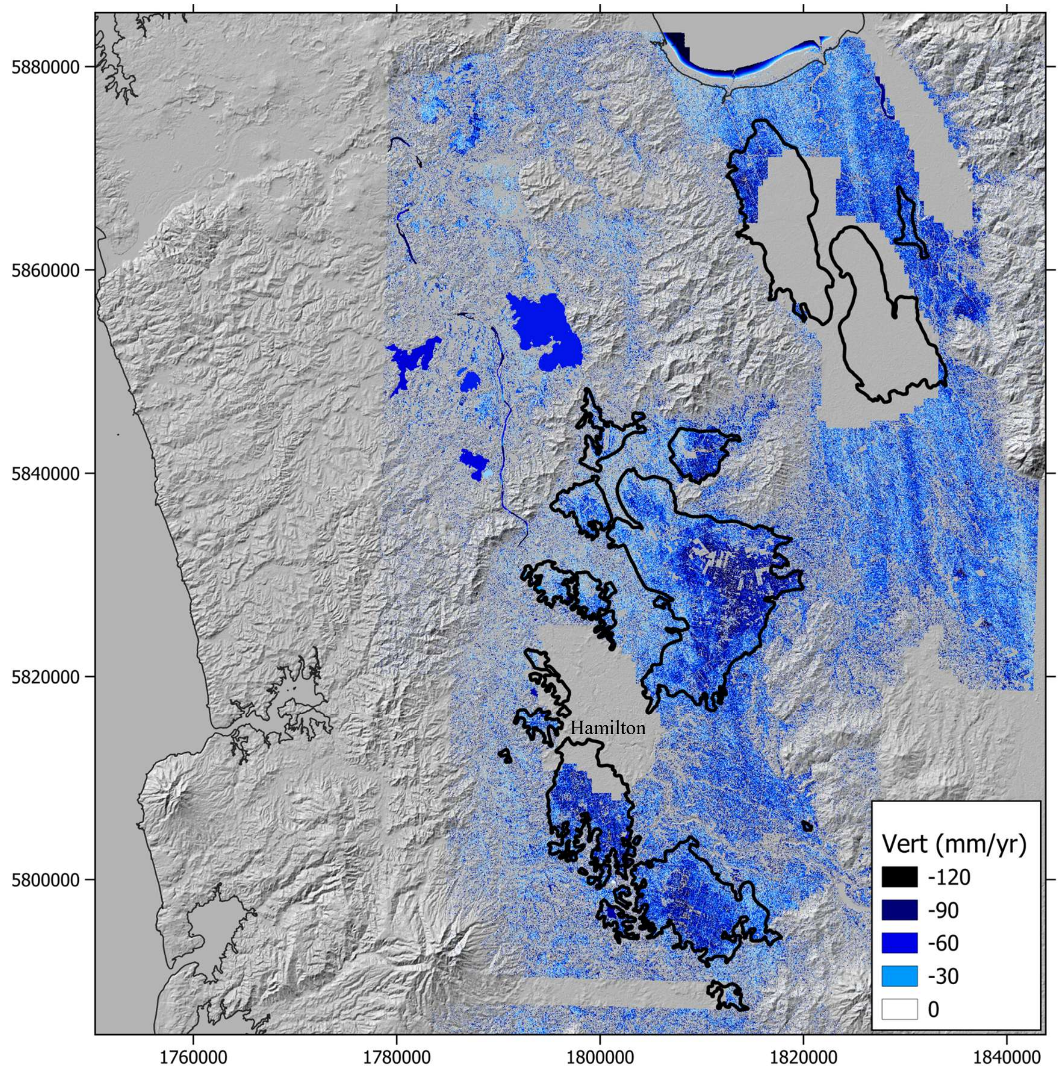

Figure 4. DEM difference map (2021 LiDAR DEM less 2013 Copernicus DEM) expressed as mean annual motion, showing strongest subsidence associated with peat soils (black boundaries), which provides independent confirmation of InSAR results (Figure 3).

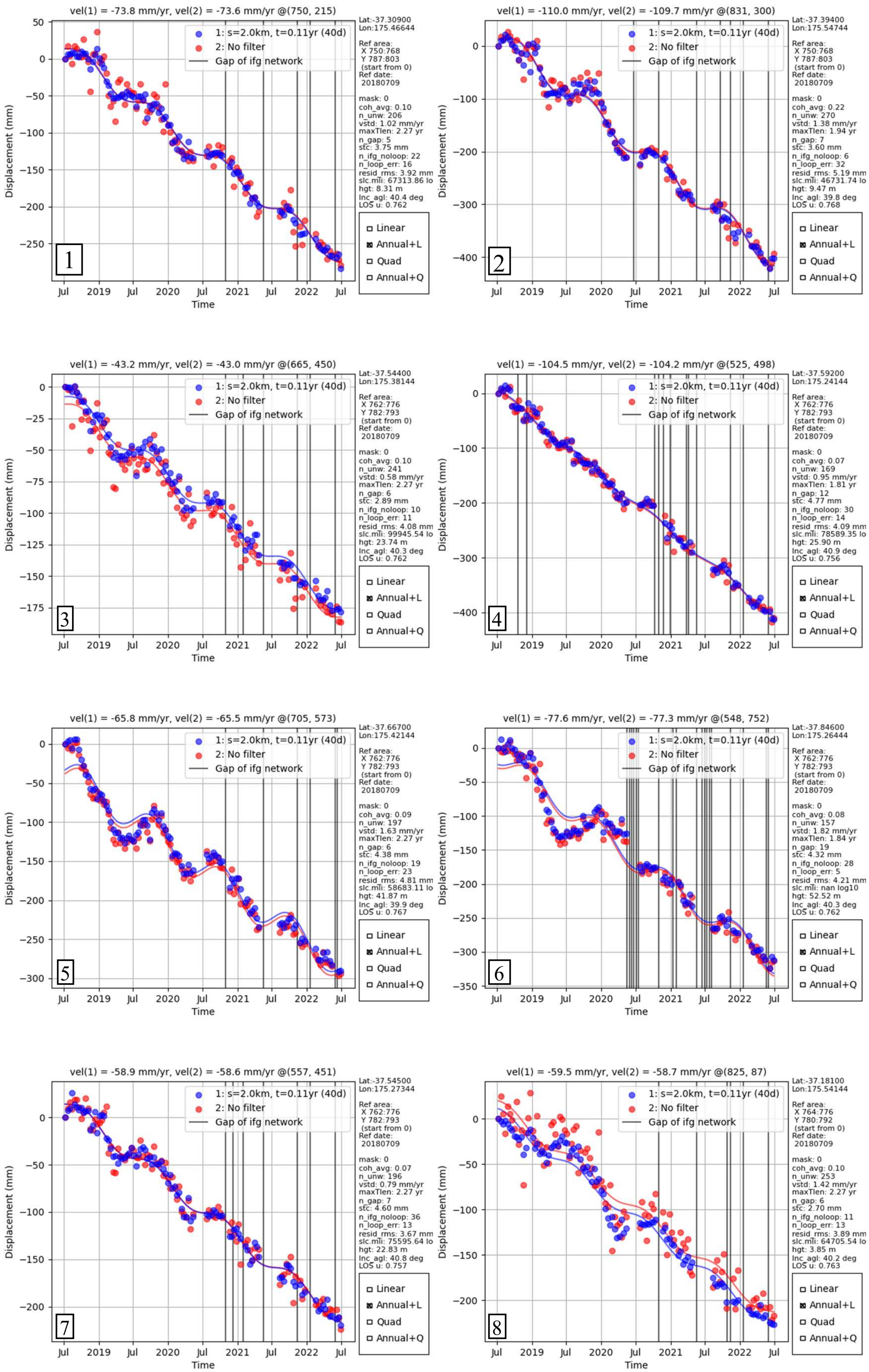

Figure 5. InSAR time series showing seasonal surface oscillation superimposed on longer term subsidence trend. Numbers correspond to locations in Figure 3.

Discussion

The observation of subsidence in the Waikato peatland soil boundaries mapped by InSAR and DEM differencing is consistent with the findings of previous studies where the causes were reported to be soil densification (shrinkage and consolidation), oxidation and physical compaction resulting from artificial drainage and other agricultural activities (Schipper and McLeod, 2002; Pronger et al., 2014; Glover-Clark, 2020; Layton, 2022) (see following section: *Subsidence Mechanisms*).

Over 80% of Waikato peatlands have now been drained for pastoral use (since the early 1900s) (Davoren, 1978; Pronger et al., 2014; Layton, 2022). This has resulted in widespread subsidence from soil densification and loss of carbon through oxidation of organic matter, with contemporary estimates of between 19 mm year^{-1} (Pronger et al., 2014) and 34 mm year^{-1} (Schipper & McLeod, 2002). The mean rate from LiCSBAS is higher (~ -40 mm year^{-1}) but may be an overestimate because of the 'fading signal' effect (see *Methods*).

Schipper & McLeod (2002) used drained and undisturbed peat soil depths at the Moanatuatua peatland (southernmost peatland in *Figure 3* and *Figure 4*) to estimate mean subsidence (-34 mm year^{-1}), which they attributed partly to densification (63%), and partly to oxidation of organic matter to the atmosphere, i.e. CO_2 degassing (37%) (2.5 to 5.0 ton C ha^{-1} year^{-1}). A more recent study at Moanatuatua based on repeated GPS measurements (2000 – 2012) provided a lower mean rate (-21 mm year^{-1}) (Pronger et al., 2014). As expected, InSAR provides a much higher mean subsidence (~ -40 mm year^{-1} vertical) in the area (2018 – 2022), and the DEM differencing estimate is even higher (~ -60 mm year^{-1}) (2013 – 2021). The uncertainty of both LiCSBAS and DEM differencing methods means both mean subsidence estimates must be regarded with caution, but the similarity of deformation maps is compelling, and provides confidence in both methods to delineate peatland areas.

Subsidence in the Waikato most concentrated within peatland soil boundaries, but there is also elevated subsidence (~ -25 mm year^{-1}) in soils with lower organic carbon content, i.e. partly mineralised gley soils of the Hauraki Plains near Ngatea and Kerepehi (*Figure 3, Figure 3 and Figure 4*). It is possible this subsidence is an artifact, or exaggerated by the fading signal effect, but interesting to note time-series for both peatland and Hauraki gley soils show seasonal peat surface oscillation (PSO) superimposed on a longer-term subsidence trend (*Figure 5*). If confirmed, subsidence on the low-lying Hauraki Plains could pose a major flood risk, so should be verified by independent methods as soon as possible. CO_2 degassing is another potential issue, as rates for partly mineralised carbon soils (i.e. gleys) are poorly constrained but may be significant (Leiber-Sauheitl et al., 2014; Eickenscheidt et al., 2015; Tiemeyer et al., 2016).

Most series show displacement maxima occur after July, which is consistent with recent PSO studies for the same peatlands and period (Glover-Clark, 2020; Layton, 2022). These studies measured the oscillation using onsite field methods and correlated shrinking/swelling of soils to seasonal dry/wet conditions. Both studies concluded the oscillation could confound derivation of longer-term subsidence rates (i.e. those based on a limited number of repeat field-based measurements); InSAR provides an advantage in this respect as mean subsidence rates are based on time series of many measurements (~12-day frequency) acquired over multiple years.

Surface drainage channels (yellow lines, *Figure 6*) clearly correspond with the subsiding peatland areas, but also the Hauraki Plains. It is interesting to note that the

Land Information New Zealand (LINZ) sourced drainage channels may underestimate the true density and extent of drainage channels (Burge et al., 2023).

Our results show that InSAR and DEM differencing provides alternate methods for mapping and measuring subsidence of peatlands and other soils at a regional scale. Extrapolation of the InSAR derived subsidence rates indicates about 1m of peat depth will be lost every 25 years. At this rate, large areas of drained peatlands in the Waikato region will be lost much sooner than was previously estimated by Pronger et al. (2014).

Deformation Mechanisms

In drained peatlands, the primary mechanisms are likely to be soil densification (shrinkage and consolidation) and oxidation. Densification may occur in surface soils where pore volumes are reduced by cycles of drying and wetting, and re-saturation after drying does not restore the soil to its original volume (hysteresis) (Elsaidy, 2021). Drainage has resulted in the shrink/swell cycling of peatland soils that were previously saturated throughout the year (Schipper and McLeod, 2002; Pronger et al., 2014; Glover-Clark, 2020; Layton, 2022). To a lesser extent, some soil compaction may occur via a volume-loss process occurring beneath surface soils in the aquifers that underlie low-relief farmland in the Waikato (Griffiths et al., 2023). When groundwater is extracted for irrigation or recharge is reduced by drainage or drought, it causes poroelastic compression of an aquifer's coarse-grained sands and gravel deposits, resulting in subsidence of the overlying surface (Murray & Lohman, 2018). Numerous InSAR studies have correlated subsidence with aquifer compaction caused by abstraction of groundwater for agriculture in arid areas (for example, Castellazzi et al., 2016; Motagh et al., 2017; Navarro-Hernández et al., 2020; Cigna and Tapete, 2021; Peng et al., 2022; Orhan et al., 2023; Lees and Knight, 2024). However, aquifer compression and subsidence in the Waikato may be more likely to result from drainage (reduced recharge to underlying aquifers) than from groundwater abstraction; aquifers lose recharge to surface streams and rivers through drainage (Rissmann et al., 2012).

Physical pressure applied by heavy agricultural equipment (e.g. tractors) or high stocking rates is another mechanism that may cause soil densification and contribute to the observed subsidence (Batey, 2009; Keller et al., 2019; Hooijer et al., 2012; Nusantra et al., 2018; Pronger et al., 2014).

Oxidation of soil organic carbon (CO_2 release) and associated subsidence is an active area of research in drained Waikato peatlands (Schipper and McLeod, 2002; Pronger et al., 2014; Glover-Clark, 2020; Campbell et al., 2021; Layton, 2022; Pronger et al., 2022) and globally (Dawson et al., 2010; Elsgaard et al., 2012; Hooijer et al., 2012; Hoogland et al., 2012; Tiemeyer et al., 2016; Nusantra et al., 2018; Hoyt et al., 2020; Que et al., 2021; Liang et al., 2024). Drainage lowers the water table, exposing organic material to oxidation, which converts it to carbon dioxide and causes subsidence (Kellner, 2003; Dawson et al., 2010; Hoyt et al., 2020). Soil organic carbon may also be dissolved and mobilised by drainage after rainfall, which provides another subsidence mechanism via mass outflow (Freeman et al., 2004; Guimarães et al. 2013; Rosset et al., 2022).

Stable Areas

The relative stability of towns compared to surrounding pastural areas may be consistent with the lack of subsidence mechanisms described in the previous section (***Deformation Mechanisms***), or may be an artifact of the fading signal effect (see **Methods**).

Assuming the former, towns insulate underlying soils because buildings, roads, and stormwater drainage prevent seasonal shrink/swell cycling from direct exposure to rainfall and sunlight. Agricultural drainage (surface and subsurface) is largely absent in towns, preventing shrinkage from dehydration. Roads are impervious to soil pore fluid exchange, indicating less dehydration from solar heating and less coupling to the atmosphere, which limits oxidation and weathering-related consolidation (Scalenghe and Marsen, 2009).

Environmental Impacts

Soil is the largest terrestrial reservoir of organic carbon, and understanding net inflows/outflows is critical for mitigation efforts (Oertel et al., 2016; Georgiou et al., 2022). Among all soil types, drained peatlands are a particularly concentrated CO_2 source (Hoyt et al., 2020; Huang et al., 2021). In New Zealand, drained organic soils, grassland, and cropland alone probably contribute between 7.6% and 9.8% of net carbon emissions (NNE), and InSAR was previously recommended as a method to map subsidence of organic soils (Pronger et al., 2022). The magnitude of these emissions and the uncertainties of current methods mean that it is critical to refine the areal extent of affected soils and associated emission factors. Where oxidation contributes to soil subsidence, InSAR-derived subsidence maps may provide a proxy for organic soils and associated NEE, allowing for improved quantification and mitigation efforts.

The health impacts of nitrate in drinking water are an active area of research in New Zealand (Richards et al., 2022; Rogers et al., 2023). Accordingly, agricultural drainage and associated contamination, especially nitrate from animal urine and mineralisation of highly productive grazing pastures, is a major issue in New Zealand (Monaghan, 2005; Collins et al., 2007; Dench & Morgan, 2021). Both open ditch (surface) and subsurface artificial drainage on farms are widespread in New Zealand (Collins et al., 2007). Such artificial drainage networks are the major conveyance systems for land use derived contaminant loss across large areas of the Waikato.

InSAR-derived subsidence maps may provide an indication of contamination source areas through the correlation between drainage and/or irrigation and soil subsidence.

Flooding is the most frequent damaging natural hazard in New Zealand (Craig et al., 2021), and climate change is expected to further increase the frequency of extreme rainfall events in New Zealand (Hughes et al., 2021; Paulik et al., 2021). This will be a major issue going forward in low-elevation coastal agricultural areas simultaneously impacted by sea level rise (Craig et al., 2023) and low-relief inland areas subject to inundation from overflowing rivers (Paulik et al., 2021; Griffin et al., 2023). Our results show moderate subsidence in low-lying coastal in the Hauraki District. Confirming subsidence in these areas should be undertaken as soon as possible to allow timely mitigation measures. The situation may be analogous to the Netherlands, where a large part of the western coastal region is covered by organic soils that were historically drained for agriculture; these areas subsided below sea level and now require extensive flood prevention measures (Hoogland et al., 2012).

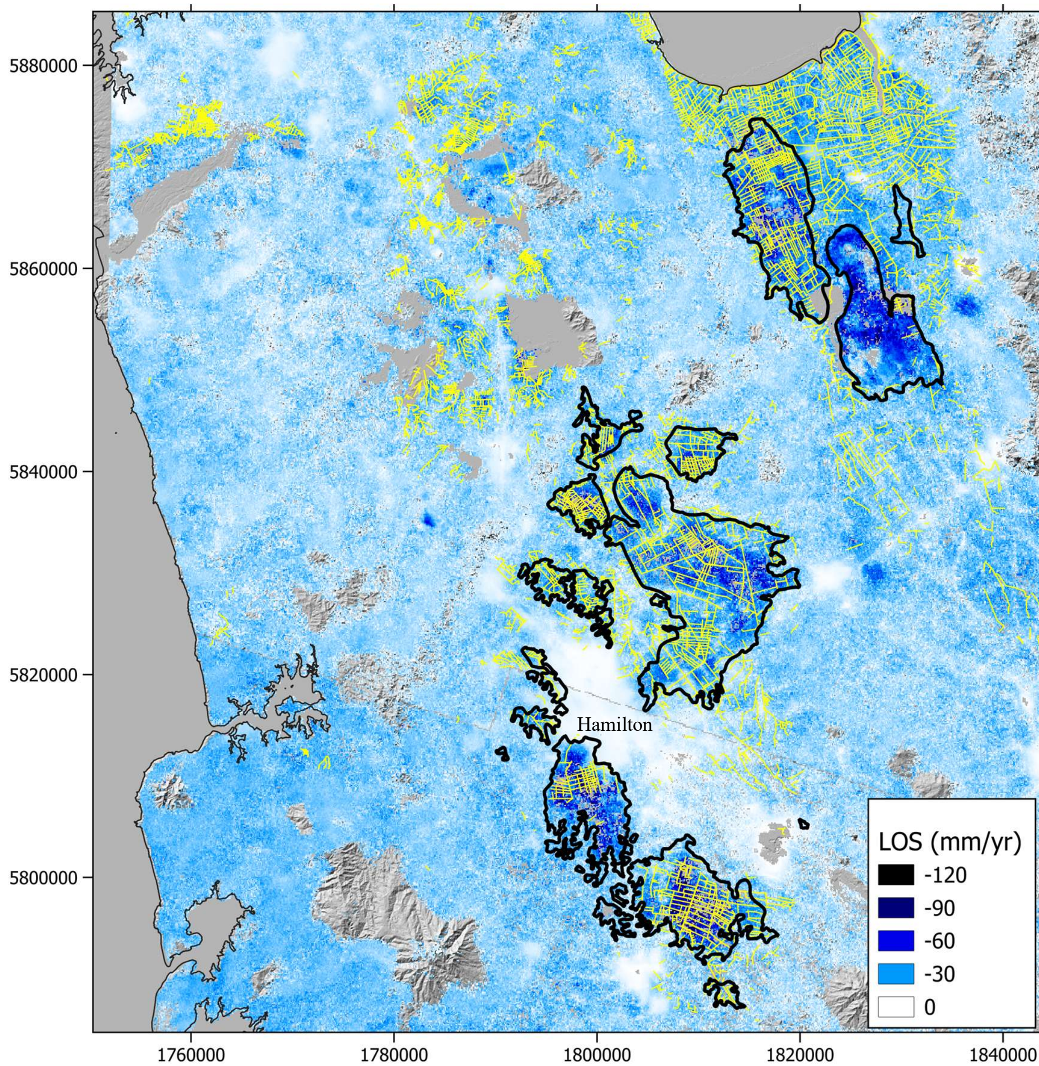

Figure 6 InSAR velocity map with peat soils (black boundaries) and agricultural surface drainage channels (thin yellow lines, Land Information New Zealand - https://data.linz.govt.nz).

Summary

Here we utilise InSAR analysis (2018-2022), and DEM differencing (2013 – 2021) to show distinct areas of subsidence in the northern Waikato Region of New Zealand are neatly contained within known peatland soil boundaries. InSAR time series show the peatlands undergo seasonal elevation changes from rainfall absorption superimposed on a longer-term subsidence trend, which agrees with previous ground-based studies.

The primary driver of subsidence is well documented - the artificial drainage of peatlands for agriculture. Our findings demonstrate that satellite-based approaches offer an efficient and scalable method for monitoring peatland subsidence across broad regions, which is not feasible with ground-based methods alone.

Widespread subsidence is also mapped across the near-sea-level Hauraki Plains, in both peat and gley soils, but the degree to which this is a processing artifact (fading signal) is unknown. If confirmed by independent methods, this is expected to be a major issue going forward as coastal areas are simultaneously impacted by sea level rise and subsidence; parts of the Hauraki Plains may become unsuitable for traditional agriculture or horticultural use.

Future land use decision-making needs to consider the social, economic and environmental consequences of the loss of peatlands, and subsidence of low-elevation farmland elsewhere, which has consequences for soil conservation, climate change mitigation, water quality, and flood risk management. Future work should include extending InSAR coverage to other regions and time periods to determine the full extent of organic soil subsidence in New Zealand. Verification of InSAR results should be undertaken using independent datasets and methods, including repeat LiDAR surveys (point cloud differencing), or conventional ground-based levelling surveys.

Acknowledgments

The authors wish to acknowledge Dr. Yu Morishita for developing the LiCSBAS tool. It is astonishing software, and this work would not have been possible without it. This paper contains modified Copernicus Sentinel data (2018–2022) downloaded from the Centre for Observation and Modelling of Earthquakes, Volcanoes and Tectonics (COMET) web portal. The authors wish to acknowledge Waikato Regional Council for their ongoing funding of InSAR studies in the Waikato.

References

Alshammari, L., Boyd, D. S., Sowter, A., Marshall, C., Andersen, R., Gilbert, P., ... & Large, D. J. (2020). Use of surface motion characteristics determined by InSAR to assess peatland conditions. Journal of Geophysical Research: Biogeosciences, 125(1), e2018JG004953.

Batey, T. (2009). Soil compaction and soil management – a review. Soil Use and Management, 25(3), 335-345. https://doi.org/10.1111/j.1475-2743.2009.00236.x

Blann, K. L., Anderson, J. L., Sands, G. R., & Vondracek, B. (2009). Effects of agricultural drainage on aquatic ecosystems: a review. Critical reviews in environmental science and technology, 39(11), 909-1001.

Burge, O. R., Price, R., Wilmshurst, J. M., Blyth, J. M., & Robertson, H. A. (2023). LiDAR reveals drains risks to wetlands have been under-estimated. New Zealand journal of ecology, 47(1), 1-9.

Campbell, D. I., Glover-Clark, G. L., Goodrich, J. P., Morcom, C. P., Schipper, L. A., & Wall, A. M. (2021). Large differences in CO2 emissions from two dairy farms on a drained peatland driven by contrasting respiration rates during seasonal dry conditions. Science of the Total Environment, 760, 143410.

Castellazzi, P., Arroyo-Domínguez, N., Martel, R., Calderhead, A. I., Normand, J. C., Gárfias, J., & Rivera, A. (2016). Land subsidence in major cities of Central Mexico: Interpreting InSAR-derived land subsidence mapping with hydrogeological data. International journal of applied earth observation and geoinformation, 47, 102-111.

Cigna, F., & Tapete, D. (2021). Satellite InSAR survey of structurally-controlled land subsidence due to groundwater exploitation in the Aguascalientes Valley, Mexico. Remote Sensing of Environment, 254, 112254.

Collins, R., Mcleod, M., Hedley, M., Donnison, A., Close, M., Hanly, J., ... & Matthews, L. (2007). Best management practices to mitigate faecal contamination by livestock of New Zealand waters. New Zealand Journal of Agricultural Research, 50(2), 267-278.

Cook, M. E., Brook, M. S., Hamling, I. J., Cave, M., Tunnicliffe, J. F., & Holley, R. (2023). Investigating slow-moving shallow soil landslides using Sentinel-1 InSAR data in Gisborne, New Zealand. Landslides, 20(2), 427-446.

Craig, H., Paulik, R., Djanibekov, U., Walsh, P., Wild, A., & Popovich, B. (2021). Quantifying national-scale changes in agricultural land exposure to fluvial flooding. Sustainability, 13(22), 12495.

Craig, H., Wild, A., & Paulik, R. (2023). Dairy farming exposure and impacts from coastal flooding and sea level rise in Aotearoa-New Zealand. International Journal of Disaster Risk Reduction, 98, 104079.

Davoren, A. (1978). A Survey of New Zealand Peat Resources. The National Water and Soil Conservation Group.

Dawson, Q., Kechavarzi, C., Leeds-Harrison, P. B., & Burton, R. G. O. (2010). Subsidence and degradation of agricultural peatlands in the Fenlands of Norfolk, UK. Geoderma, 154(3-4), 181-187.

Dench, W. E., & Morgan, L. K. (2021). Unintended consequences to groundwater from improved irrigation efficiency: Lessons from the Hinds-Rangitata Plain, New Zealand. Agricultural Water Management, 245, 106530.

Eickenscheidt, T., Heinichen, J. & Drösler, M. (2015). The greenhouse gas balance of a drained fen peatland is mainly controlled by land-use rather than soil organic carbon content. Biogeosciences 12, 5161–5184.

Elsaidy, H. (2021). Effect of Wetting and Drying Cycles on the 3D Hydromechanical Behaviour of Expansive Residual Soils in Auckland (Doctoral dissertation, ResearchSpace@ Auckland).

Elsgaard, L., Görres, C. M., Hoffmann, C. C., Blicher-Mathiesen, G., Schelde, K., & Petersen, S. O. (2012). Net ecosystem exchange of CO2 and carbon balance for eight temperate organic soils under agricultural management. Agriculture, ecosystems & environment, 162, 52-67.

Ewers, R. M., Kliskey, A. D., Walker, S., Rutledge, D., Harding, J. S., & Didham, R. K. (2006). Past and future trajectories of forest loss in New Zealand. Biological conservation, 133(3), 312-325.

Farr, T. G., & Kobrick, M. (2000). Shuttle Radar Topography Mission produces a wealth of data. Eos, Transactions American Geophysical Union, 81(48), 583-585.

Freeman, C., Fenner, N., Ostle, N. J., Kang, H., Dowrick, D. J., Reynolds, B., ... & Hudson, J. (2004). Export of dissolved organic carbon from peatlands under elevated carbon dioxide levels. Nature, 430(6996), 195-198.

Georgiou, K., Jackson, R. B., Vindušková, O., Abramoff, R. Z., Ahlström, A., Feng, W., ... & Torn, M. S. (2022). Global stocks and capacity of mineral-associated soil organic carbon. Nature communications, 13(1), 3797.

Glover-Clark, G. (2020). Spatiotemporal variability of hydrology in Moanatuatua drained peatland and its influence on CO_2 emissions and surface oscillations (Doctoral dissertation, The University of Waikato).

Griffin, C., Wreford, A., & Cradock-Henry, N. A. (2023). 'As a farmer you've just got to learn to cope': Understanding dairy farmers' perceptions of climate change and adaptation decisions in the lower South Island of Aotearoa-New Zealand. Journal of Rural Studies, 98, 147-158.

Griffiths, J., Yang, J., Woods, R., Zammit, C., Porhemmat, R., Shankar, U., ... & Howden, N. (2023). Parameterization of a National Groundwater Model for New Zealand. Sustainability, 15(17), 13280.

Guimarães, D. V., Gonzaga, M. I. S., da Silva, T. O., da Silva, T. L., da Silva Dias, N., & Matias, M. I. S. (2013). Soil organic matter pools and carbon fractions in soil under different land uses. Soil and Tillage Research, 126, 177-182.

Hamling, I. J., Williams, C. A., & Hreinsdóttir, S. (2016). Depressurization of a hydrothermal system following the August and November 2012 Te Maari eruptions of Tongariro, New Zealand. Geophysical Research Letters, 43(1), 168-175.

Hamling, I.J. (2020). InSAR observations over the Taupō Volcanic Zone's cone volcanoes: insights and challenges from the New Zealand volcano supersite. New Zealand Journal of Geology and Geophysics, pp.1-11.

Hamling, I. J., Wright, T. J., Hreinsdóttir, S., & Wallace, L. M. (2022). A snapshot of New Zealand's dynamic deformation field from Envisat InSAR and GNSS observations between 2003 and 2011. Geophysical Research Letters, 49 (2), e2021GL096465.

Harvey, M.C., K. M. Luketina, McLeod, J., and Rowland, J.V. (2019). Geothermal Subsidence and Inflation in Taupo: A Comparison of Detection Methods. Proceedings 40th New Zealand Geothermal Workshop.

Harvey, M. (2021). Sentinel-1 InSAR captures 2019 catastrophic White Island eruption. Journal of Volcanology and Geothermal Research, 411, 107124.

Hewitt, A. E., Balks, M. R., & Lowe, D. J. (2021). The Soils of Aotearoa New Zealand. Berlin/Heidelberg, Germany: Springer.

Hoogland, T., Van den Akker, J. J. H., & Brus, D. J. (2012). Modeling the subsidence of peat soils in the Dutch coastal area. Geoderma, 171, 92-97.

Hooijer, A., Page, S., Jauhiainen, J., Lee, W. A., Lu, X. X., Idris, A., & Anshari, G. (2012). Subsidence and carbon loss in drained tropical peatlands. Biogeosciences, 9(3), 1053-1071.

Hoyt, A. M., Chaussard, E., Seppalainen, S. S., and Harvey, C. F. (2020). Widespread subsidence and carbon emissions across Southeast Asian peatlands. Nature Geoscience, 13(6), 435-440.

Hrysiewicz, A., Williamson, J., Evans, C. D., Jovani-Sancho, A. J., Callaghan, N., Lyons, J., ... & Holohan, E. P. (2024). Estimation and validation of InSAR-derived surface displacements at temperate raised peatlands. Remote Sensing of Environment, 311, 114232.

Huang, Y., Ciais, P., Luo, Y., Zhu, D., Wang, Y., Qiu, C., Goll, D.S., Guenet, B., Makowski, D., De Graaf, I. and Leifeld, J., 2021. Tradeoff of CO2 and CH4 emissions from global peatlands under water-table drawdown. Nature Climate Change, 11(7), pp.618-622.

Hughes, J., Cowper-Heays, K., Olesson, E., Bell, R., & Stroombergen, A. (2021). Impacts and implications of climate change on wastewater systems: A New Zealand perspective. Climate Risk Management, 31, 100262.

Ingebritsen, S., C. Mcvoy, B. Glaz, and Park, W. (1999). Florida Everglades: Subsidence threatens agriculture and complicates ecosystem restoration. In: D. Galloway, D. Jones, and S. Ingebritsen, editors, Land subsidence in the United States. USGS, Reston, VA. p. 95–106.

Keller, T., Sandín, M., Colombi, T., Horn, R., & Or, D. (2019). Historical increase in agricultural machinery weights enhanced soil stress levels and adversely affected soil functioning. Soil and Tillage Research, 104293. https://doi.org/10.1016/j.still.2019.104293.

Kearse, J. (2024). InSAR Measurement of Vertical Land Motion at Urban and Rural New Zealand Coastal Strips (Doctoral dissertation, Open Access Te Herenga Waka-Victoria University of Wellington).

Kellner, E. (2003). Wetlands-different types, their properties and functions.

Layton, H. G. (2022). Peat soil properties and seasonal surface elevation changes of drained Waikato peatlands (Master Thesis, The University of Waikato).
Lees, M., & Knight, R. (2024). Quantification of record-breaking subsidence in California's San Joaquin Valley. Communications Earth & Environment, 5(1), 677.
Leiber-Sauheitl, K., Fuß, R., Voigt, C., & Freibauer, A. (2014). High CO2 fluxes from grassland on histic Gleysol along soil carbon and drainage gradients. Biogeosciences, 11(3), 749-761.
Liang, Z., Hermansen, C., Weber, P. L., Pesch, C., Greve, M. H., de Jonge, L. W., ... & Elsgaard, L. (2024). Underestimation of carbon dioxide emissions from organic-rich agricultural soils. Communications Earth & Environment, 5(1), 286.
Maghsoudi, Y., Hooper, A. J., Wright, T. J., Lazecky, M., & Ansari, H. (2022). Characterizing and correcting phase biases in short-term, multilooked interferograms. Remote Sensing of Environment, 275, 113022.
Manzo, M., Ricciardi, G. P., Casu, F., Ventura, G., Zeni, G., Borgström, S., ... & Lanari, R. (2006). Surface deformation analysis in the Ischia Island (Italy) based on spaceborne radar interferometry. Journal of Volcanology and Geothermal Research, 151(4), 399-416. J. Volcanol. Geotherm. Res. 151 (4), 399–416.
Monaghan, R. M., & Smith, L. C. (2004). Minimising surface water pollution resulting from farm-dairy effluent application to mole-pipe drained soils. II. The contribution of preferential flow of effluent to whole-farm pollutant losses in subsurface drainage from a West Otago dairy farm. New Zealand Journal of Agricultural Research, 47(4), 417-428.
Monaghan, R. M., Paton, R. J., Smith, L. C., Drewry, J. J., & Littlejohn, R. P. (2005). The impacts of nitrogen fertilisation and increased stocking rate on pasture yield, soil physical condition and nutrient losses in drainage from a cattle-grazed pasture. New Zealand Journal of Agricultural Research, 48(2), 227-240.
Morishita, Y., Lazecky, M., Wright, T. J., Weiss, J. R., Elliott, J. R., & Hooper, A. (2020). LiCSBAS: An open-source InSAR time series analysis package integrated with the LiCSAR automated Sentinel-1 InSAR processor. Remote Sensing, 12(3), 424.
Motagh, M., Shamshiri, R., Haghighi, M. H., Wetzel, H. U., Akbari, B., Nahavandchi, H., ... & Arabi, S. (2017). Quantifying groundwater exploitation induced

subsidence in the Rafsanjan plain, southeastern Iran, using InSAR time-series and in situ measurements. Engineering geology, 218, 134-151.

Murray, K. D., & Lohman, R. B. (2018). Short-lived pause in Central California subsidence after heavy winter precipitation of 2017. Science Advances, 4(8), eaar8144.

Navarro-Hernández, M. I., Tomás, R., Lopez-Sanchez, J. M., Cárdenas-Tristán, A., & Mallorquí, J. J. (2020). Spatial analysis of land subsidence in the San Luis potosi valley induced by aquifer overexploitation using the coherent pixels technique (CPT) and sentinel-1 insar observation. *Remote Sensing*, *12*(22), 3822.

Nusantra, R. W., Hazriani, R., & Suryadi, U. S. (2018). Water table depth and peat subsidence due to land use change of peatlands. Presented at the IOP Conference Series: Earth and Environmental Science.

Oertel, C., Matschullat, J., Zurba, K., Zimmermann, F., & Erasmi, S. (2016). Greenhouse gas emissions from soils—A review. Geochemistry, 76(3), 327-352.

Orhan, O., Haghshenas Haghighi, M., Demir, V., Gökkaya, E., Gutiérrez, F., & Al-Halbouni, D. (2023). Spatial and Temporal Patterns of Land Subsidence and Sinkhole Occurrence in the Konya Endorheic Basin, Turkey. Geosciences, 14(1), 5.

Paulik, R., Crowley, K., Cradock-Henry, N. A., Wilson, T. M., & McSporran, A. (2021). Flood impacts on dairy farms in the Bay of Plenty Region, New Zealand. *Climate*, *9*(2), 30.

Peng, M., Lu, Z., Zhao, C., Motagh, M., Bai, L., Conway, B. D., & Chen, H. (2022). Mapping land subsidence and aquifer system properties of the Willcox Basin, Arizona, from InSAR observations and independent component analysis. Remote Sensing of Environment, 271, 112894.

Pronger, J., Schipper, L. A., Hill, R. B., Campbell, D. I., & McLeod, M. (2014). Subsidence rates of drained aricultural peatlands in New Zealand and the relationship with time since drainage. Journal of Environmental Quality, 43(4), 1442-1449.

Pronger, J., Glover-Clark, G., Price, R., Campbell, D., & Schipper, L. (2022). Improving accounting of emissions from drained organic soils. New Zealand Ministry of Primary Industries Technical Paper No: 2023/16.

Qiu, C., Ciais, P., Zhu, D., Guenet, B., Peng, S., Petrescu, A. M. R., ... & Brewer, S. C. (2021). Large historical carbon emissions from cultivated northern peatlands. Science advances, 7(23), eabf1332.

Richards, J., Chambers, T., Hales, S., Joy, M., Radu, T., Woodward, A., ... & Baker, M. G. (2022). Nitrate contamination in drinking water and colorectal cancer: Exposure assessment and estimated health burden in New Zealand. Environmental research, 204, 112322.

Rissmann, C., Wilson, K., & Hughes, B. (2012). Waituna catchment groundwater resource. Environment Southland Technical Report, Publication, (2012-04).

Rogers, K. M., van der Raaij, R., Phillips, A., & Stewart, M. (2023). A national isotope survey to define the sources of nitrate contamination in New Zealand freshwaters. Journal of Hydrology, 617, 129131.

Rosset, T., Binet, S., Rigal, F., & Gandois, L. (2022). Peatland dissolved organic carbon export to surface waters: Global significance and effects of anthropogenic disturbance. Geophysical Research Letters, 49(5), e2021GL096616.

Scalenghe, R., & Marsan, F. A. (2009). The anthropogenic sealing of soils in urban areas. Landscape and Urban Planning, 90(1), 1-10. https://doi.org/10.1016/j.landurbplan.2008.10.011.

Schipper, L.A., and McLeod, M. (2002). Subsidence rates and carbon loss in peat soils following conversion to pasture in the Waikato Region, New Zealand. Soil Use Manage. 18:91–93. doi:10.1111/j.1475-2743.2002.tb00225.x

Tampuu, T., Praks, J., De Zan, F., Kohv, M., & Kull, A. (2023). Relationship between ground levelling measurements and radar satellite interferometric estimates of bog breathing in ombrotrophic northern bogs. Mires and Peat, 29.

Tiemeyer, B., Albiac Borraz, E., Augustin, J., Bechtold, M., Beetz, S., Beyer, C., ... & Zeitz, J. (2016). High emissions of greenhouse gases from grasslands on peat and other organic soils. Global change biology, 22(12), 4134-4149.

Xu, Z., Jiang, L., Niu, F., Guo, R., Huang, R., Zhou, Z., & Jiao, Z. (2022). Monitoring regional-scale surface deformation of the continuous permafrost in the qinghai–tibet plateau with time-series InSAR analysis. Remote Sensing, 14(13), 2987.

Figure Captions

Figure 1. Waikato study location overlaid on SRTM DEM (Farr & Kobrick, 2000). Cross hatching indicates peat soil areas (https://lris.scinfo.org.nz/layer/119585-s-map-soil-classification-soilorder-aug-2024/).

Figure 2. LiCSBAS masking parameters. Numbers shown in the parentheses next to the titles of each noise index are the applied threshold value. See Morishita et al. (2020) for full explanation of masking thresholds.

Figure 3. InSAR velocity map showing subsidence associated with peat soils (black boundaries). Numbers show time series locations (Figure 5).

Figure 4. DEM difference map (2021 LiDAR DEM less 2013 Copernicus DEM) expressed as mean annual motion, showing strongest subsidence associated with peat soils (black boundaries), which provides independent confirmation of InSAR results (Figure 3).

Figure 5. InSAR time series showing seasonal surface oscillation superimposed on longer term subsidence trend. Numbers correspond to locations in Figure 3.

Figure 6. InSAR velocity map with peat soils (black boundaries) and agricultural surface drainage channels (thin yellow lines, Land Information New Zealand - https://data.linz.govt.nz).